

# Covert Scanning of Low Signature Targets Using High Speed Photon-Counting

A. McCarthy, R. J. Collins, P. A. Hiskett, C. S. Parry, V. Fernandez,  
S. Hernandez-Marin, A. M. Wallace and G. S. Buller  
School of Engineering and Physical Sciences, Heriot-Watt University,  
Riccarton, Edinburgh, EH14 4AS

## Abstract

*This paper describes a scanning time-of-flight system which uses the time-correlated single photon-counting technique to produce three-dimensional depth images of scenes using low light levels. The data for the scene is acquired using a scanning optical system and a single optimised detector. Depth information on a low contrast scene at a distance of 330 metres has been successfully acquired.*

Keywords: Single-photon counting, Three-dimensional scanning, Avalanche photodiodes

## Introduction

The technique of time-correlated single-photon counting has been used since the 1960's, mainly for the measurement of fast, low-level light signals in, for example, time-resolved fluorescence measurements. The technique measures the time difference (or "micro-time") between an optical input pulse (typically a repetitive laser signal) and a photon event recorded by a single-photon detector. Over many laser pulses, a histogram of the number of photon counts versus micro-time can result in a statistically accurate representation of the actual optical transient signal being measured [1]. In this project, we have developed a scanning system based on the time-of-flight approach which uses a pulsed diode laser source and semiconductor-based single-photon avalanche diode detectors. The system scans a scene in the horizontal and vertical and builds up a 3-dimensional image of the depth. The time-gating and high sensitivity of the time-correlated single-photon counting (TCSPC) approach offers the potential for low light level and eye-safe operation.

## System Overview

The time-of-flight system developed in this project uses a pair of galvanometer mirrors to scan a scene and build up a 3-dimensional image of the depth. The mirrors are used to (a) scan the laser output over the scene and (b) direct the collected return scattered light to a single optimised single-photon counting detector. This is in contrast to the alternative approach of imaging onto an array of single-photon detectors [2] where parallel readout-out remains a major technological obstacle. In addition, the single-photon counting arrays that are currently available suffer significantly from the deleterious effects of crosstalk between pixels, performance non-uniformity and a general use of non-optimised single-photon detectors. The scanning approach permits the use of a single high-speed data acquisition module, and the modular construction easily facilitates the use of alternative optimised single-photon detectors, as they become available.

The prototype uses state-of-the-art commercially available components and a schematic diagram of the scanning system is shown in Figure 1. The key elements are:

- **Computer:** This is used to run the custom software, developed in this project, which controls hardware for both the scanning of the scene and the data acquisition process. It processes the acquired data and enables the user to configure relevant system parameters.

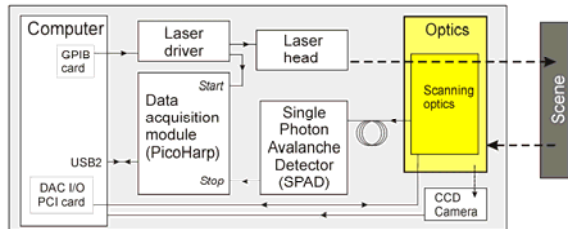


**Figure 1:** Schematic diagram showing the key components of the system for the covert scanning of low signature targets using high-speed photon-counting.

- **Laser head and laser driver:** the collimated output of an 842 nm wavelength edge emitting picosecond pulsed laser diode is used to illuminate the scene. The laser and the driver generate low output power pulses, of  $\leq 50 \mu\text{W}$ , at repetition rates varying from 5 to 80 MHz. These are commercially available components available from several vendors.
- **Single-photon avalanche detector (SPAD):** For the work done so far, a commercially available, fibre-coupled module from Perkin-Elmer with a jitter of approximately 400 ps has been used. The modularity of the system does mean that

other fibre-pigtailed shallow-junction Si SPADs with jitter of  $<100 \text{ ps}$ , can be easily tested, as they become available.

- **Data acquisition module:** The PicoHarp unit from PicoQuant is connected to the electrical output from the SPAD. This facilitates high photon-counting acquisition rates with minimal deadtime ( $<95 \text{ ns}$ ) after photon events.
- **Optics:** The optics in the sensor head enable a scene to be scanned with the laser output, as well as imaging the return photons onto a single-mode fibre core. The scanning is achieved by using a pair of galvanometer mirrors operated in a closed loop configuration, under computer control.

### Optical Design of System

A general layout diagram of the optical system is shown in Figure 2. An appropriate commercially available SLR camera lens (interchangeable) acts as the system objective. The objective is used to direct the outgoing laser to the target and also to efficiently collect the scattered photons returned from the target. Both the outgoing laser beam and the return photons are scanned using galvanometer mirrors – meaning that a single optimised

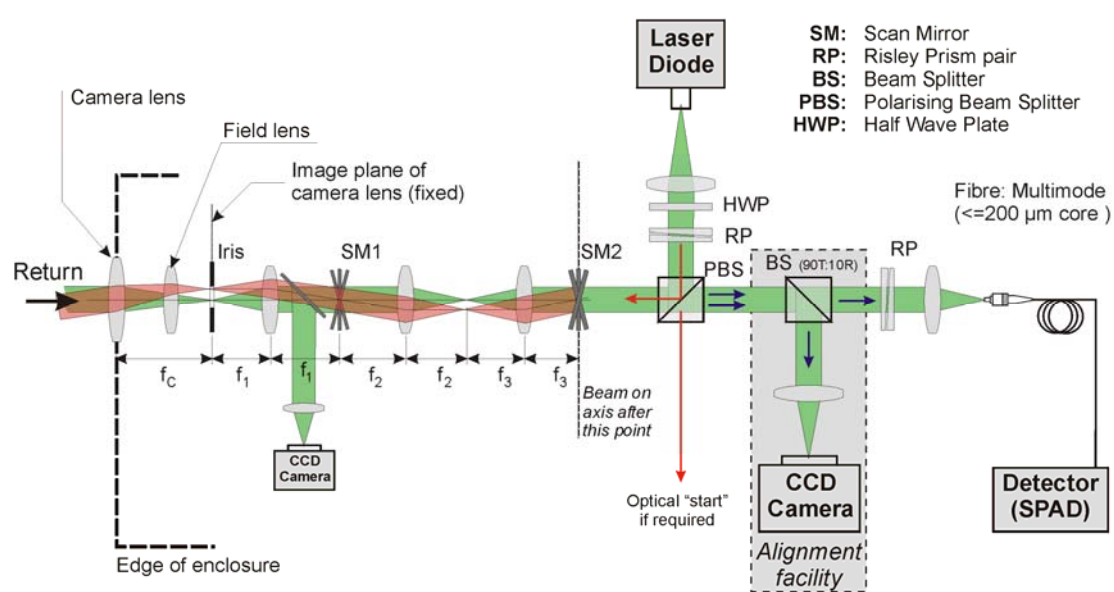


**Figure 2:** This schematic shows the optical layout of the system.

photon-counting detector can be used. Polarisation optics is used to discriminate the outgoing target, and returning signal, beams. The required part of the image of the scene formed by the objective is relayed “pixel” by “pixel” onto the fibre core (which is connected to the SPAD) via the imaging optics and computer controlled galvo mirrors. The scanning mirrors, SM1 and SM2, and the required lenses are arranged in a spatially separated telecentric relay configuration. This arrangement requires more lenses and thus a greater optomechanical footprint when compared to alternative schemes but it is more exact optically, permitting spatial filtering of background illumination using a small diameter optical fibre core connected to the detector channel.

In this sensor, the field-of-view of the scanned image is largely determined by the field-of-view of the image presented to the internal system optics by the objective lens. The actual spatial resolution achieved depends on a number of factors including the focal lengths of the lenses, the aberrations of the optics and in particular the size of the fibre core coupled to the detector. When the system had been aligned and focussed on the scene, the

aperture of the receive channel when using a 9 µm core fibre was estimated to be 50 mm in diameter at 330 m with the transmit channel beam diameter being slightly larger. This equates to a spatial resolution of ~200 mm at 1 km range and corresponds to the minimum angular step resolution determined by the galvos.

### Optomechanics

The sensor head consists of a custom-built optomechanical assembly which uses the slotted baseplate approach, depicted in Figure 3, for mounting the majority of the optical components. An appropriate network of slots of a fixed width is machined in a plate of suitable material. The optical components, or devices, are mounted in cylindrical steel barrels, placed in the slot as shown and held in position with magnets thus providing a convenient semi-kinematic mount. The recent baseplates designed, manufactured and used in recent years at Heriot-Watt University have been standardised to the dimensions indicated in the figure.

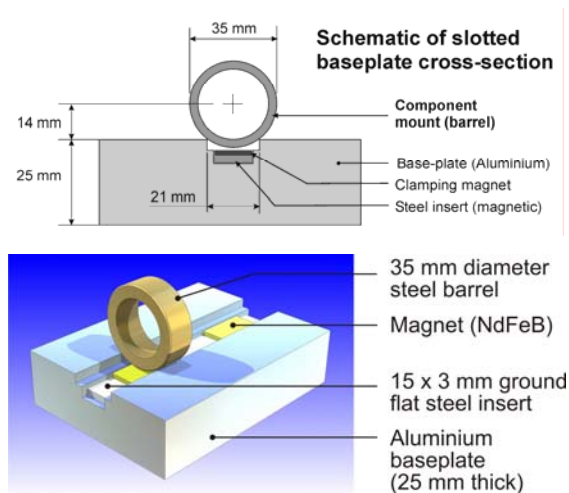


**Figure 3:** The diagrams show a cross-sectional schematic and a 3D CAD image of a slotted baseplate and a component mount.

The objective (camera) lens was attached to the side of the baseplate using an adaptor plate – this enables the lens to be easily changed. The completed sensor head measured ~275 x 275 x 170 mm high. The entire optomechanical assembly was modelled using the SolidEdge 3D CAD program and the post processing carried out using EdgeCAM.

### Software

A complete software package has been developed as part of the project for controlling the system and analysing the acquired data. The processing software is divided into two parts, a LabVIEW program (which includes a graphical user interface (GUI)) and a C program which performs the data analysis.

The LabVIEW program allows the user to set relevant system control parameters such as the laser pulse repetition frequency, size of scan area, number of pixels, etc and displays the resulting depth profile. In addition, the LabVIEW program handles communication with the galvo mirrors which control the beam position, the PicoHarp 300 time-correlated single-photon counting electronics and the laser driver.

Two forms of data acquisition have been trialed: “move-stare-move-stare” and continuous scan. The “move-stare” technique moves the galvo mirrors to a particular pixel before activating the laser, acquiring the data using the PicoHarp 300, deactivating the laser and moving to the next pixel. A separate file of detector and synchronisation events is generated on the backing storage of the computer for each pixel. This technique is inefficient as there is a communications handshaking delay involved with control of the laser and the PicoHarp 300.

In a continuous scan, the laser and PicoHarp 300 are activated once at the start of the measurement and the galvo mirrors are constantly in motion during the experiment – as shown in Figure 4. This results in one file which contains all of the detector and synchronisation events for the entire scene. Low temporal resolution markers are introduced into the detector event data via TTL inputs from a front panel D plug connection on the PicoHarp 300 to signify the end of each line. The C program is called by the LabVIEW program and handles the processing of the raw detector event records recorded by the PicoHarp 300 into a depth profile. For the data from “move-stare” measurements, each file of detector and synchronisation events is converted into a histogram and a simple cross correlation algorithm used to determine the position of the peak corresponding to the return from the target. The data from continuous scan measurements is first subdivided into lines using the low resolution markers. Each line is further subdivided into segments of equal duration corresponding to the individual pixels. To remove any ambiguity in range which may be introduced by the motion of the galvo mirrors, a normalised Gaussian weighting profile in time is applied to the detector events for each pixel. Counts which occur early or late in the duration of one pixel are assigned a lower (non integer) value than

those from the middle of each pixel duration when the histogram is constructed. The resulting histogram (which will contain non-integer bin values) is then analysed using the same simple cross correlation algorithm as in the analysis of the experiments performed using “move-stare”.

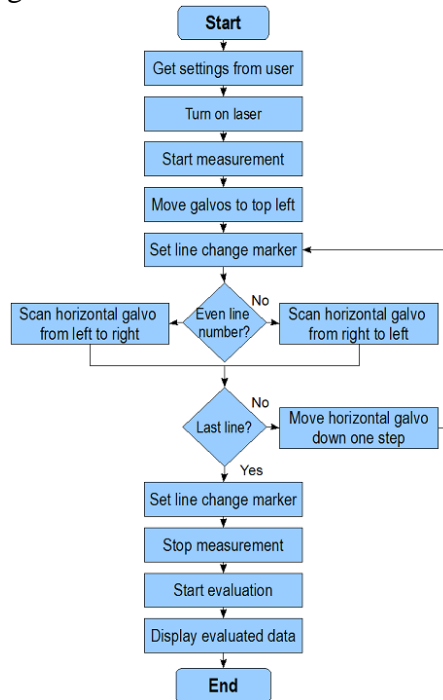


**Figure 4:** *The continuous scan technique*

### Scan Results

Scans were carried out over ranges of 30 metres (internal corridor, see Figure 6) and 330 metres (outdoor range at HWU) prior to 1.4 km trials at Porton Down. These scans were all done with an f/2.8, 200 mm focal length objective lens. The alignment of the transmit and receive channels was checked on the 30 m, 330 m and 1.4 km ranges and found to be very good. The aperture of the receive channel was estimated to be 50 mm in diameter at 330 m with the transmit channel beam diameter being slightly larger. The results of the scan done on the 330 m outdoor range shown in Figure 7(a) were very impressive – the curvature of the (non-cooperative) ~600 mm diameter concrete

pillars was clearly visible, as shown in Figure 7(b) below.

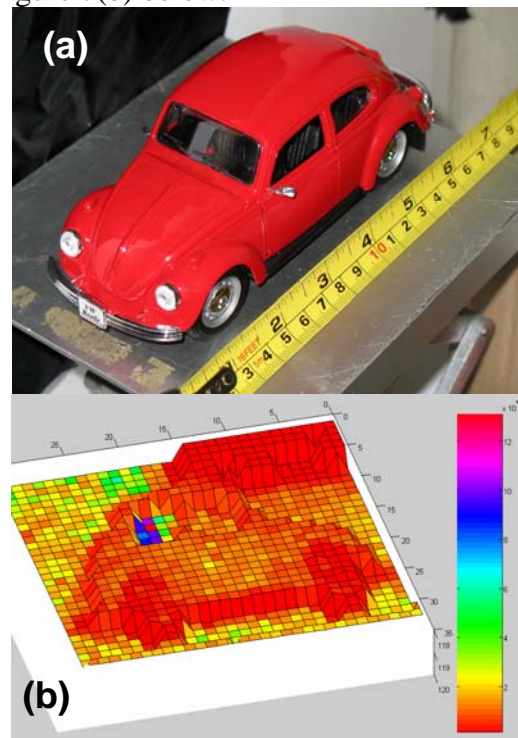


**Figure 6:** (a) *Photograph of 1:24 scale model car* (b) *Depth-intensity scan result at 30 metres (intensity key shown on right side of plot).*

### Further Data Analysis Algorithms for Future Work

The cross correlation algorithm is only capable of detecting a target return which is clearly distinct from the noise. Future versions of the analysis software will use more complex algorithms such as matched filter and reversible jump Markov chain Monte Carlo (RJMCMC) algorithms [3] specifically aimed at processing the photon count data from the scanning sensor developed under this project.

Matched filtering is carried out in an efficient way using the Fast Fourier Transform (FFT) algorithm implemented in the frequency domain as this is faster than a typical correlation algorithm [4]. As

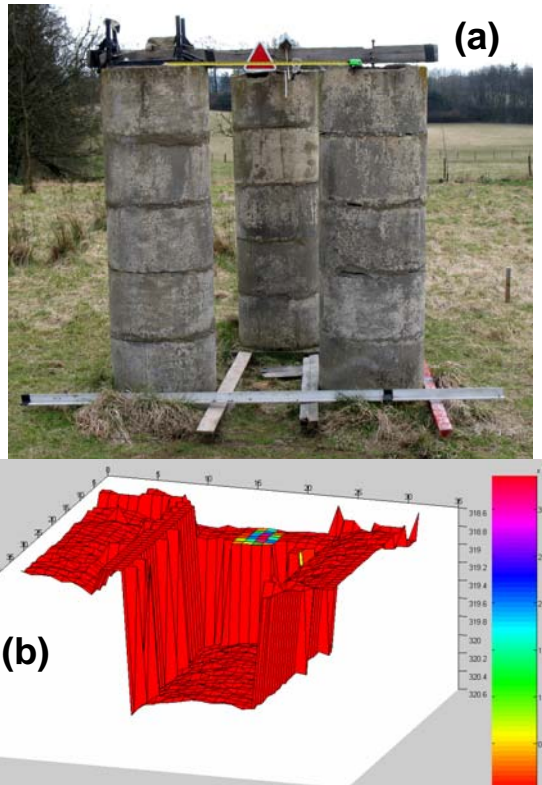


Figure 7: (a) Photograph of the concrete pillar structure on the 330 metre range at Heriot-Watt. (b) Depth-intensity scan: Note the depth scan shows the curvature of the pillars (approximate radius of curvature 30 cm), whilst the small retro-reflective element is evident from its increased intensity of return (see intensity key on right side of plot).

opposed to RJMCMC algorithms, this approach only gives estimates of the plausible position of the returns. No information at all is given on the uncertainty of these estimates and this approach is likely to fail for small signal-to-noise ratios. Hybrid software/hardware FFTs algorithms can be designed to improve the estimates and to assess uncertainty. Hardware approaches will include the development of specialised digital signal processors (DSPs) to perform certain mathematical operations. Software approaches include hybrid FFT/MCMC algorithms in which the initial values for the MCMC algorithm are given by the FFT algorithm. This will reduce a-priori the number of iterations needed in the MCMC algorithm.

In this paper, we do not deal with the possible hardware solutions to this problem but we focus on the software development. To that end, we have analysed and combined some of these algorithms to optimise the trade-off between speed and accuracy. As the goal of this work is to achieve sub-second processing per image, the choice of the “optimum” algorithm depends on a trade-off between complexity (accuracy) and execution time.

Initial results on synthetic data show that the simplest algorithm that meets the particular time constraints of this project is matched filtering using FFTs. The accuracy of depth measurement on synthetic data (and real data from other sensors) is satisfactory, provided the return can be detected by a suitable threshold, and the execution time for an image of 32 x 32 elements is about 2 seconds according to the different timing and profiling results. This is greater than, but comparable to, the specification of 1 second. The problem of this “excessive” execution time can be handled in one of three different ways. First, for two signals of length  $N$ , the complexity of the FFT matched filtering algorithm is of the order of  $3N \log_2 N$ , thus reducing the length of the signals (currently 4096 time samples), is certainly feasible. Given a-priori knowledge of the position of signal return, this would reduce the processing time with no loss of depth resolution. Second, we could use a computer or other processor designed for digital signal processing (DSP). Third, instead of using the modified version of the FFT algorithm described by [5], we could use other commercial FFT libraries such as the Intel Math Kernel Library (MKL) 9.0 which is composed of highly optimized mathematical functions for math, engineering, scientific and financial applications requiring high performance on Intel platforms. Yet another option is the FFTW (the acronym FFTW comes from “Fastest Fourier Transform in the West”)

developed by Frigo and Johnson [6] at the MIT Laboratory for Computer Science which suggests significant improvements are possible, even on general purpose machines. A particularly strong feature of the FFTW is the ability to run tests on a particular sized array on a particular processor. These tests determine the fastest method to compute the transform, and this knowledge can be stored in a file or string for later use. Given a large number of transforms to be computed, all of the same size, this method yields a worthwhile gain in speed compared to the default case when FFTW uses a heuristically chosen algorithm. FFTW is licensed under the GNU General Public License. It is also licensed commercially by MIT and is used in the Matlab functions which compute FFTs.

We conclude with the following considerations:

- The FFT matched filter is the only one that will process a 32 x 32 at ~1 frame per second given pure software and the current PC specification.
- If more accuracy is needed, multiple peaks are considered or assessment on the uncertainty of the data is required, RJMCMC algorithms are preferred. However, they are considerably more complex.
- To reduce the execution time, significant hybrid software/hardware design is required.
- The execution time might be reduced if we developed real-time versions of (RJ)MCMC algorithms using parallel and embedded software. To date, there are very few approaches to parallelising them.

### **Avoidance of Range Ambiguity**

A major issue in high repetition frequency time-of-flight systems is that of range ambiguity, where the arrival times are incorrectly synchronised with outgoing laser pulses to give the possibility of a non-

unique depth measurements. In order to completely avoid the possibility of ambiguity, we must restrict the laser repetition frequency such that only one pulse is in transit at one time. Of course, at a one kilometre range the round-trip transit time is 6.67  $\mu$ s, restricting the laser pulse frequency to less than 150 kHz. Such a low repetition rate will greatly reduce the rapidity of range data collection and the effectiveness of the overall photon-counting time-of-flight technique. Hence, for kilometre-range photon-counting time-of-flight to fulfil its potential in terms of short duration acquisition times, it is vital to address this range ambiguity issue.

Recently [7], we have performed experiments using an alternative technique which utilises a non-periodic pulse train. The demonstration of this technique used a pseudorandom sequence of laser pulses at a 1 GHz clock frequency with, on average, one tenth of the available time windows occupied by a laser pulse. The received pattern was correlated with the transmitted pattern to identify the unique target time-of-flight time. In these demonstrations, a GHz VCSEL source was used and was pulsed using a GHz pulse pattern generator using a repeated random pattern of length 96000 bits. The range measurements were made at an approximate range of 330 m using cooperative targets. The approach used a commercial Si single-photon avalanche diode detector and the detector events were recorded using a time-stamping board (TSB). A single reference pulse was used to synchronise the TSB and each detector event was time-stamped with respect to this pulse. To accurately maintain synchronisation, the laser driver and the TSB are phased-locked using an external clock, in this case a 10 MHz rubidium clock. By performing correlation of the transmitted and received signals, accurate correlation patterns were found which showed unambiguous depth measurements to centimetre resolution at a range of 330 metres. Figure 8 shows a

correlations for seven different positions of a target at positions of 5, 10, 25, 40, 50, 60 cm with respect to a reference correlation which is also shown. The measured range of a number of target positions is plotted against calculated target position is shown in Figure 9. It is clear that unambiguous range data is found with depth resolution of several centimetres.

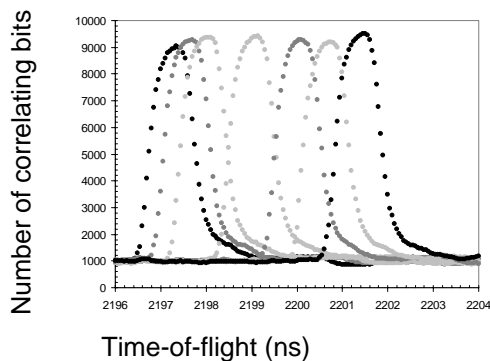


**Figure 8** A graph of number of correlations against time-of-flight for 7 different positions of a (moveable) corner cube at a range of 330 metres. The corner cube positions were at a zero reference, 5, 10, 25, 40, 50 & 60 cm. The measurements were obtained using steps of 50 ps.

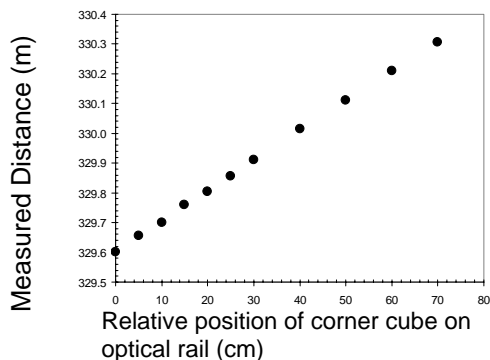


**Figure 9** A graph of the measured range using the pattern recognition against the relative position of only the moveable corner cube on the optical rail.

### Conclusion

This paper describes the first scanning time-of-flight system which utilises the time-correlated single-photon counting technique, in conjunction with data

analysis algorithms, to produce three-dimensional depth images of scenes using very low laser power levels. The demonstrator system used an individual optimised single-photon detector and was constructed using a novel slotted baseplate approach which facilitates testing using with alternative component selection whilst maintaining the optomechanical stability necessary for lab and field trials.

The system has an xy resolution of 25 cm at a distance of 1 km, with a depth resolution of at least that figure. A number of depth scans have been performed whilst characterising the system, although the issue of solar background remains the limiting factor. Future work will concentrate on reducing the solar background issue with a combination of improved spatial and spectral filtering, whilst a full characterisation of the system will take place using alternative optical components. Further work will be done on the selection and implementation of the optimised algorithm for low contrast return signals using actual experimental data.

### References

1. G.S. Buller and A.M. Wallace “Recent advances in Ranging and Three-Dimensional imaging using time-correlated single-photon counting” IEEE Journal of Selected Topics in Quantum Electronics, vol. 13, pp1006-1015, (2007)
2. B. Aull, “3D Imaging with Geiger-mode Avalanche Photodiodes”, Optics and Photonics News (May 2005)
3. S. Hernandez-Marin, A. M. Wallace, and G. J. Gibson. “Bayesian Analysis of Lidar Signals with Multiple Returns”, to be published in IEEE PAMI, 2007.
4. J. Jan. “Digital Signal Filtering, Analysis and Restoration”, IEE Telecommunications Series 44, 2000.
5. W. H. Press, S. A. Teukolsky, W. T. Vetterling, and B. P. Flannery. “Numerical Recipes in C: The Art of

*Scientific Computing*". Cambridge University Press, New York, NY, USA, 1992.

6. M. Frigo and S. G. Johnson. "*FFTW: An adaptive software architecture for the FFT*". In Proc. 1998 IEEE Intl. Conf. Acoustics Speech and Signal Processing, volume 3, pages 1381–1384. IEEE, 1998.
7. Philip A. Hiskett, Colin S. Parry, Aongus McCarthy and Gerald S. Buller, "*A photon-counting time-of-flight ranging technique developed for the avoidance of range ambiguity at gigahertz clock rates*", Submitted to Optics Express (March 2008)

### **Acknowledgements**

The work reported in this paper was funded by the Electro-Magnetic Remote Sensing (EMRS) Defence Technology Centre, established by the UK Ministry of Defence and run by a consortium of SELEX Galileo, Thales UK, Roke Manor Research and Filtronic.

